Pore-Scale Monitoring of the Effect of Microarchitecture on Fungal Growth in a Two-Dimensional Soil-Like Micromodel

Raghad Soufan[1], Yolaine Delaunay[2], Laure Vieublé Gonod[1], Leslie M. Shor[3], Patricia Garnier[2], Wilfred Otten[4] and Philippe C. Baveye[1]*

[1] UMR EcoSys, AgroParisTech, Université Paris-Saclay, Thiverval-Grignon, France, [2] UMR EcoSys, Institut National de la Recherche Agronomique, Université Paris-Saclay, Thiverval-Grignon, France, [3] Department of Chemical and Biomolecular Engineering, University of Connecticut, Mansfield, CT, United States, [4] School of Water, Energy and Environment, Cranfield University, Cranfield, United Kingdom

In spite of the very significant role that fungi are called to play in agricultural production and climate change over the next two decades, very little is known at this point about the parameters that control the spread of fungal hyphae in the pore space of soils. Monitoring of this process in 3 dimensions is not technically feasible at the moment. The use of transparent micromodels simulating the internal geometry of real soils affords an opportunity to approach the problem in 2 dimensions, provided it is confirmed that fungi would actually want to propagate in such artificial systems. In this context, the key objectives of the research described in this article are to ascertain, first, that the fungus *Rhizoctonia solani* can indeed grow in a micromodel of a sandy loam soil, and, second, to identify and analyze in detail the pattern by which it spreads in the tortuous pores of the micromodel. Experimental observations show that hyphae penetrate easily inside the micromodel, where they bend frequently to adapt to the confinement to which they are subjected, and branch at irregular intervals, unlike in current computer models of the growth of hyphae, which tend to describe them as series of straight tubular segments. A portion of the time, hyphae in the micromodels also exhibit thigmotropism, i.e., tend to follow solid surfaces closely. Sub-apical branching, which in unconfined situations seems to be controlled by the fungus, appears to be closely connected with the bending of the hyphae, resulting from their interactions with surfaces. These different observations not only indicate different directions to follow to modify current mesoscopic models of fungal growth, so they can apply to soils, but they also suggest a wealth of further experiments using the same set-up, involving for example competing fungal hyphae, or the coexistence of fungi and bacteria in the same pore space.

Keywords: hyphae, spread, microfluidics, fungal highway, microscale

INTRODUCTION

An estimated 1.5 million species of fungi are present in terrestrial ecosystems (Hawksworth, 2001) where they fulfill a wide array of essential ecological functions, in particular in the global carbon cycle (Cromack and Caldwell, 1992). Their role in soil-plant feedback processes in the rhizosphere is widely regarded as key to achieving the estimated 100% increase in overall food production that will be needed in the next 25 years, amidst decreasing availability of suitable land and already overexploited surface- or groundwater resources (e.g., Sposito, 2013; Baveye, 2015; Baveye et al., 2018).

To maximize the benefits that can be derived from the involvement of fungi in these different contexts, we can rely on a wealth of qualitative information about these organisms. For centuries, it has been known that fungal colonies grow as an interconnected network of hyphae, collectively referred to as mycelium (Fricker et al., 2017). In soils, fungal hyphae absorb and mineralize stable biomolecules like cellulose or lignin. Since they can access organic matter and nutrients located in much tinier pores than those typically accessible to plant roots, fungi are able to provide sustenance that otherwise would be difficult for over 90% of vascular plants to take up on their own (Boddy, 1993). Many soil-borne fungi are pathogenic to plants, severely reducing crop production worldwide (Fisher et al., 2012), whereas others have antagonistic properties, or hyperaccumulate metal contaminants, making them particularly suited to remediate polluted soils (Stamets, 2005). Last in this quick overview, but certainly not least, fungi play a crucial role in stabilizing the architecture of soils (e.g., Miller and Jastrow, 2000).

Underpinning these ecologically important processes is the ability of fungi to invade the very convoluted pore space in heterogeneous soil environments, with its tortuous paths, multiple constrictions, and in some cases dead end spaces, all of which may be variably filled with water (Otten et al., 2001; Pajor et al., 2010). Tremendous technological advances over the last two decades, in particular the development of advanced X-ray computed tomography (CT) scanners, now allow the geometrical features of the pore space in which fungal hyphae grow to be determined at resolution of a few microns, which are adequate given typical widths of hyphae of the order of 3–17 μm. Various computer models have been developed in the last decade, which use this information derived from CT images to predict the spread of fungal biomass in soils (e.g., Falconer et al., 2012, 2015; Cazelles et al., 2013). These models predict the amount of fungal biomass that is likely to be present locally in the pore space, and their outputs appear reasonable in light of the few macroscopic observations available. These models have proven very useful to understand the possible effects of various soil parameters, e.g., the connectivity and tortuosity of the pore space, on the proliferation of fungi or the interaction of competing fungal species in soils.

In a number of situations, for example during the bioclogging of soils (e.g., Baveye et al., 1998) or when trying to understand how the presence of fungal hyphae could affect the retention and transport of water in soils, not just the amount of fungal biomass likely to be present locally, but also the precise location and configuration of fungal hyphae in soil pores, may have

a significant influence on processes of interest. Unfortunately, the only experimental information available to us at this point, at the microscopic scale, about the growth pattern of fungal hyphae in soil pores has not evolved much in the last 30 years. Some progress has been made in the 3D visualization of the configuration of fungal hyphae in systems constituted of polystyrene beads (Lilje et al., 2013) or in wood. Recent advances in the visualization of root hairs of similar diameter as fungi in small samples using synchrotron X-ray CT does demonstrate that at least in very small samples visualizing fungi might be possible (Koebernick et al., 2017). It is however noted that relative to the scale of fungal colonies and over which nutrient can be translocated such sample sizes would not be representative to capture colony development. Therefore, in actual soils, the only way to visualize fungal hyphae is through snapshots that one can get after preparing soil thin sections (e.g., Harris et al., 2002, 2003), or stabilizing soil samples for electron microscopy (e.g., Foster, 1988). The resulting images provide us with very useful information about hyphae and what surrounds them at discrete locations in soils at specific instants of time. However, it has been so far impossible to derive from these snapshots a reliable picture of the environmental and morphological parameters that control the 3-dimensional path followed by individual fungal hyphae in soil pores. Some fungi, like *Rhizoctonia solani,* exhibit a remarkably constant, undoubtedly genetically-determined behavior when grown in Petri dishes, with virtually constant branching angles and average internodal distances (Boswell and Hopkins, 2008; Boswell and Davidson, 2012; Hopkins and Boswell, 2012; Choudhury et al., 2018). It is tempting to assume that the same characteristics are exhibited when this organism grows in the pore space of a soil, but there is no reason at this point to believe that this assumption is warranted. In fact, it seems safe to take as a working hypothesis that the frequent presence of obstacles in the path of the spreading hyphae in soils is likely to modify significantly the behavior of *R. solani* compared to what it is in Petri dishes. Indeed is has been shown that colony geometry is to a large extent determined by connected tortuous pathways on soil (Otten and Gilligan, 1998; Otten et al., 1999). Following Watts et al. (1998), one might for example assume that fungal hyphae in soils are likely to manifest some type of thigmotropism, by which they would tend to remain in contact with solid surfaces after they encountered them during their foraging in the soil pore space.

Direct dynamic observations of the spread of fungal hyphae in soils are clearly direly needed, to find out to what extent the spreading and branching patterns of fungal hyphae in soils differ from those on Petri dishes. At the moment, the best opportunity we have to get a glimpse of the dynamics of hyphae in soil pores appears to be in two dimensions, by using so-called micromodels or microfuidic devices (e.g., Karadimitriou and Hassanizadeh, 2012; Stanley et al., 2016). Various authors (Hanson et al., 2006; Held et al., 2010, 2011; Hopkins and Boswell, 2012), a few years back, have used micromodels to visualize the spread of fungi. Their micromodels had rectilinear pores intersecting at right angle and of a width just a little bigger than that of hyphae. Since these early investigations, the design and manufacture of micromodels have evolved

noticeably. It is now possible to replicate faithfully the pore geometry of soils, using an inexpensive and biocompatible polymer, polydimethylsiloxane (PDMS), that offers excellent optical clarity. Deng et al. (2015) and Rubinstein et al. (2015) have used such a soil-like micromodel to observe the effect of bacterial activity on water or particle retention and movement in larger pores. Similar work with fungal hyphae has yet to be carried out.

In this general context, the key objective of the research described in the present article was to find out, apparently for the first time, if micromodels can indeed be used to monitor the growth of fungi in confined pore spaces similar to those found in soils, and to elucidate the mechanisms that control this growth. *R. solani* was selected as the target organism in part for the fact that it does not produce spores, which would complicate the dynamics, and for its remarkably predictable behavior in unconfined situations, but also because its growth in Petri dishes is described with particularly striking realism by a computer model developed by Hopkins and Boswell (2012) and extended recently to three dimensions (Vidal-Diez de Ulzurrun et al., 2017). The key ingredients of this model are briefly outlined in the section that follows this introduction, and serve as a guide later on to determine to what extent the growth pattern of hyphae observed in the microcosms differs from the "normal" 2-dimensional behavior out in the open. The article concludes with a quick overview of the many perspectives the preliminary results obtained so far open up for future experimental research and modeling.

THEORETICAL ASPECTS

In the model of Hopkins and Boswell (2012), the mycelium is thought of as a network of inter-connected tubes (representing hyphae) through which various substances (including carbon, nitrogen, trace metals, and tip vesicles) are translocated as part of an internal cytoplasm. Hyphae are modeled as a discrete series of straight line segments. After every time interval of length Δt, the local substrate concentration changes due to translocation, uptake and diffusion. New line segments are included in the fungal network, corresponding to the processes of lengthening of existing tubes (apical extension), and creation of new tubes (subapical branching), according to a set of stochastic rules that depend in part on the local concentrations of internal substrate. A further transformation of the hyphal network may result from the fusion of hyphae that come into contact with each other, a process known as anastomosis. Hopkins and Boswell's (2012) model involves many aspects related to the translocation of chemicals or materials inside the hyphae, as well as a description of the response of hyphal tips to external gradients of an inhibitor produced by the fungus itself, and which diffuses in the surrounding medium. The components of the model that interest us most here, however, are related to parameters that control the elongation and branching of the hyphae.

Apical extension is represented schematically by the creation of a new (virtual) line segment of nominal length Δx that extends from the unconnected end of an existing line segment and represents the movement of the hyphal tip over a discrete time interval Δt. In addition to different tropisms associated with gradients in nutrient- or inhibitor concentrations, hyphal tips

also display small stochastic variations in their growth axis. To simulate the process of tip movement, a "velocity-jump" model is used, which basically assumes that the velocity of hyphal tip undergoes a biased circular random walk with its orientation remaining the same or changing by an angle $\pm\Delta\theta$ (termed a velocity jump) between successive time intervals and where the localized concentration of the inhibitor induces bias so that model tips have a tendency to move in the direction of lower inhibitor concentrations, according to detailed mathematical formulas for the probability of tip re-orientation by an angle $\Delta\theta$, clockwise or anti-clockwise.

Sub-apical branching is modeled by the creation of new line segments emerging from the ends of existing line segments. Since turgor pressure is thought to be implicated in the branching process (Gow and Gadd, 1995; Riquelme and Bartnicki-Garcia, 2004), the model assumes that in the time interval Δt, the probability of an existing line segment k to generate a new line segment from its end position is zero unless the internal substrate concentration exceeds a critical concentration β. The new line segment is oriented at an angle $\pm\phi$ relative to the existing line segment with equal probability (Paulitz and Schroeder, 2005), and the internal substrate is uniformly divided between the existing and the new line segment.

Hopkins and Boswell (2012) parameterize their model with data from the literature, relative to *R. solani*. The hyphal line segment length Δx and the angular step size $\Delta\theta$ are taken to be 50 μm and $\pi/12$ radians (9°), respectively, following Riquelme et al. (1998). The branching angle ϕ is considered to be normally distributed, with mean of 79.2° and a standard deviation of 3.16°. This value of the branching angle may seem a little low, since many authors have pointed out that *R. solani* branches at right angle (90°). Nevertheless, the lower value adopted by Hopkins and Boswell (2012) has been borne out by recent experimental data. The very detailed monitoring of the growth of several fungi in Petri dishes over a 75 h timeframe, carried out by Vidal-Diez et al. (2015) using image analysis techniques, indicates that hyphae of *R. solani* branch at an angle that is in fact slightly lower than 90°, at 81.93 ± 1.15°. Nevertheless, the small standard deviation shows that it is still reasonable to view this value as virtually constant over time. The same feature seems to be also manifested by a parameter, the internodal length, which is not involved in Hopkins and Boswell's (2012) model, but is straightforward to measure in images of fungal hyphae. It corresponds to the average distance between septa (internal cross-walls separating cells in the hyphae). Vidal-Diez et al. (2015) report that the internodal length of *R. solani* first decreases from 175 to 171 μm over the first 17 h of growth, then increases stepwise to reach 180 μm at the end of 75 h. Overall, the average internodal distance they report is 179.29 ± 11.27 μm.

MATERIALS AND METHODS
Micromodel Concept and Fabrication

The microfluidic device, or micromodel, concept adopted in this research, as well as its manufacturing, have been described in detail in the recent article by Deng et al. (2015), which contains full references to earlier work as well as equipment information. To make the present article as self-contained as

possible, we shall reproduce here some information on the design and manufacturing of the micromodels. The original, much more thorough description of Deng et al. (2015) should however be consulted to obtain complete specifications.
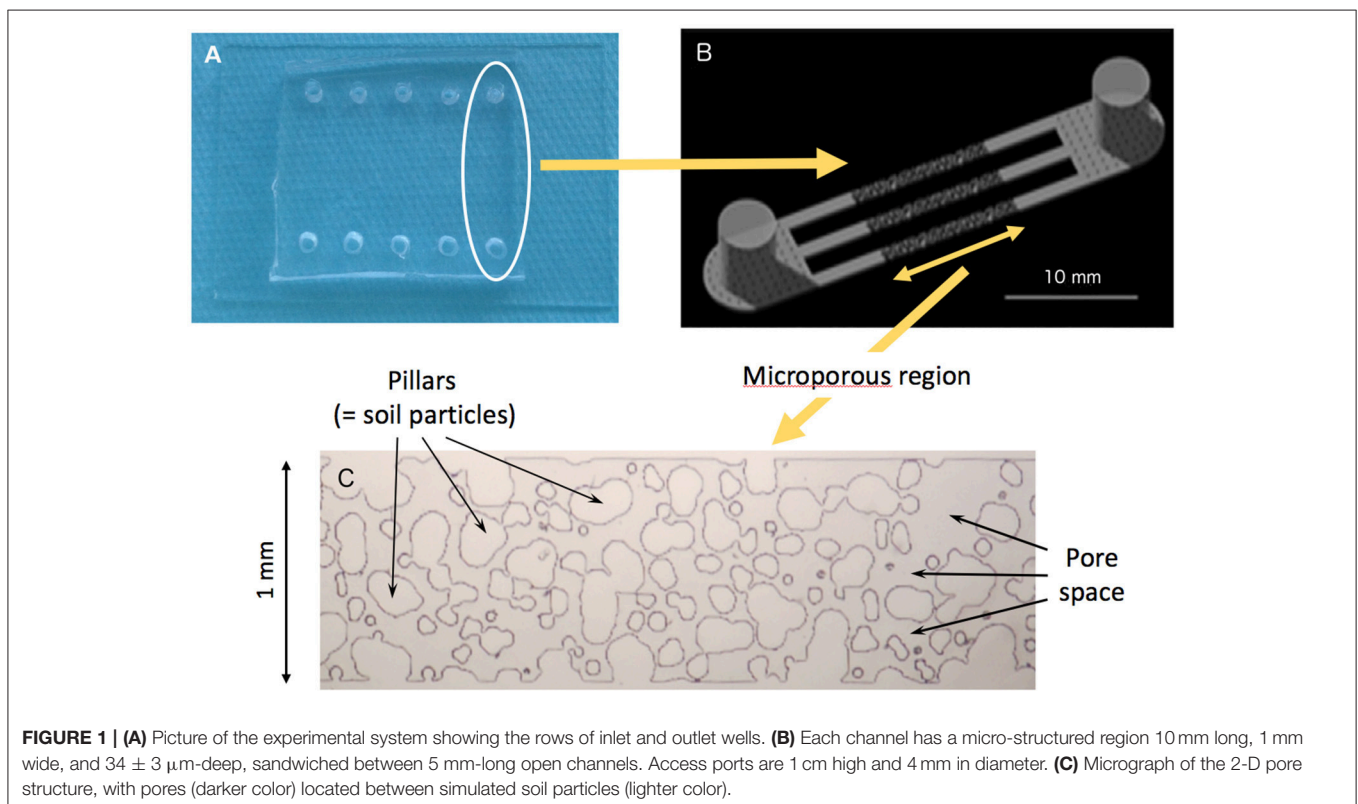
In a nutshell, each micromodel is comprised of three parallel channels each one mm wide and $34\,\mu m$ high connected to a single inlet well and a single outlet well (**Figures 1A,B**). The central, 10-mm long portion of each of the channels consists of a microstructured region, with pillars of varying sizes and shapes representing a two-dimensional slice of the solid phase of a simulated sandy loam soil (**Figure 1C**). The geometry of the microstructured region is based on a realistic computer-generated three-dimensional packing of ellipsoidal particles. The size distribution of the particles is based on an experimentally-determined sandy loam particle size distribution comprised of 56% fine sand and 44% very fine sand (USDA size ranges: 125–250 mm and 50–125 mm, respectively).

To create the soil geometry, ellipsoidal particles were randomly placed in a three-dimensional computational domain, and the packing algorithm DigiPac (Jia and Williams, 2001) was employed to create realistic particle-particle contacts. Then, a two-dimensional slice of the packed three-dimensional domain with a suitable level of pore connectivity was selected. The selected slice was then manually traced using the Raster Design toolset in AutoCAD 2010 and partitioned to completely fill the 1 mm x 10 mm microstructured region in a high-resolution chrome on-glass photomask. The geometrical features of the pseudo-2D soil pattern are as follows: particle diameters averaged 110 μm and ranged from 10 to 300 μm, and the hydraulic pore radius averaged 44 μm and ranged from 16 to 130 μm. In contrast with typical porosities of sandy loam soils, which are in the range of 25–35%, the porosity of Deng's et al. (2015) pseudo-2D emulated soil micromodel is 57%. This increase in porosity is a result of selecting in the simulated porous medium a slice that maintains pore connectivity in 2-D.

The photomask described above was then used to fabricate the reusable casting mold, called the "master," via photolithography. First, a thin layer of SU-8 2025 photoresist was spin-coated onto a 4-inch diameter Si wafer. The thickness of the photoresist coating was $34 \pm 3\,\mu m$ as determined by profilometry. Then, the photoresist was patterned by selectively exposing transparent regions in the photolithography mask to 26.4 $mWcm^{-2}$ ultraviolet light for 6.1 s then finished by cross-linking and developing steps. Finally, the master was "silanized," or coated with (tridecafluoro-1,1,2,2-tetrahydrooctyl)trichlorosilane.

Individual emulated soil micromodels were cast 1 cm thick in PDMS. First, Sylgard 184 base and curing agent were mixed in a 10:1 ratio, degassed at −75 kPa gage for 30 min, then poured over the master and cured at 60°C for 4 h. Cured castings were carefully peeled from the master (silanization facilitates release of the cured PDMS from the master), trimmed, and access ports were manually punched from the patterned side using a 4 mm biopsy punch. Finally, each casting was treated with O_2 plasma for 45 s in an evacuated air atmosphere and irreversibly bonded featured-side down to a clean glass microscope slide. The plasma treatment is desirable in order for the micromodels to better

FIGURE 1 | (A) Picture of the experimental system showing the rows of inlet and outlet wells. **(B)** Each channel has a micro-structured region 10 mm long, 1 mm wide, and $34 \pm 3\,\mu m$-deep, sandwiched between 5 mm-long open channels. Access ports are 1 cm high and 4 mm in diameter. **(C)** Micrograph of the 2-D pore structure, with pores (darker color) located between simulated soil particles (lighter color).

emulate soil since it results in PDMS having a surface charge similar to quartz sand (Roman and Culbertson, 2006), at least as long as the surface of the PDMS remains covered by water. Observations made by Cruz et al. (2017) suggests that the plasma treatment and the emulation of quartz-like surface chemistry are not permanent under unsaturated conditions. In such cases, the macromolecular mobility of the polymer at room temperature allows re-configuration at the surface, and the latter is relatively likely to have properties typical of untreated PDMS.

Cultivation of *R. solani* and Inoculation of Poppy Seeds

Potato dextrose agar (PDA) plates were inoculated with an anastomosis group (5) isolate of *R. solani* and incubated for 3 days at 23°C. Small plugs were cut from the edge of the plates and used as a source of inoculum. Following the inoculation technique adopted by Otten et al. (2012), poppy seeds (*Papaver rhoeas*) were autoclaved twice at 120°C at 1.1 Atm for 1 h over a 48 h period. Sterilized seeds were subsequently sprinkled over the PDA plates previously colonized by *R. solani*, and incubated at 23°C for 3 days.

Operation of Micromodels

The microporous portions of the channels were partially filled with sterile distilled water by injecting a small amount of water inside the access well on one side of the micromodel, and letting the water diffuse in the microporous region over time. Inspection under the microscope was used to determine, for each amount of distilled water applied, the portion of the channel porosity that was saturated.

Once the microporous region had reached equilibrium in terms of the water phase, colonized seeds were removed from the Petri dishes with the PDA, and were placed inside the access wells on the other side of the micromodel, relative to the access wells used to inject water. At this stage, the micromodel was introduced in a sterile Petri dish to maintain a suitable moisture level, but at the same time allow the exchange of oxygen and carbon dioxide with the atmosphere. The Petri dish was incubated for an initial period of 24 h before the microscopic observation of the fungal hyphae began.

Microscopy and Image Processing

Fungal spread in the channels of the micromodels was observed with a Brunel inverted light microscope (Brunel Microscope Limited, Wiltshire, U.K.). Pictures of the hyphae were typically collected as time series at regular intervals, usually one frame every 4 min. at selected locations, before the lens was repositioned on a different spot in the micromodel.

To enhance the quality and contrast of the images obtained with the light microscope, and allow easier visualization of the hyphae, the micrographs showing features of interest were processed with the imaging software Photoshop (Adobe Systems, San José, California), by selecting the green channel in the RGB format and changing its contrast setting. In some cases, false colors were added with an image analysis software (GIMP) to the liquid phase and to the simulated solid particles of the micromodels, in order to make it clearer where the fungal hyphae spread.

RESULTS AND DISCUSSION

Spread of Hyphae in the Inlet Portion of the Micromodels

Prior to the experiments, it was not clear at all that *R. solani* would manifest any inclination to enter the 34 μm-high inlet section in the micromodels, leading to the microporous region (see **Figure 1**). Our expectation, encouraged by the opinion of several experts we consulted, was that *R. solani* would prefer to stay in the much roomier access well where the poppy seed was deposited, and would have to be enticed to go inside the channel inlet section. This enticement could in principle be carried out in a number of ways, for example via a piece of fresh wood placed in the opposite access well. Based on Fries (1973) observations, the release of volatile compounds by the wood, which would diffuse through the partially saturated microporous section, might be enough of an incentive for the hyphae to penetrate the micromodel. Another option would be to add a source of dissolved carbon to the distilled water injected inside the micromodel, which would have attracted the fungus.

As it turns out, the hyphae do not need any kind of incentive to penetrate the micromodels. Evidence indicates that they do so easily and spread readily away from the poppy seeds, into the inlet portion of the micromodels, and eventually in the microporous sections as well. Near the poppy seeds (**Figure 2a**), branching tends to be abundant, and anastomosis is frequent, making it difficult to determine the range of values exhibited for the branching angle, the hyphal line segment, or the intermodal distance. Close to the entrance of the microporous portion of the micromodel (**Figure 2b**), whenever *Rhizoctonia* does not grow along the wall of the cavity, the branching pattern is very similar to what was observed earlier in the PDA agar plates, which itself was in line with accounts published in the literature. In **Figure 2b**, hyphae, with a constant width of 7 μm, branch at angles of 62, 63, 78, and 63°, respectively, from bottom to top. Branching systematically occurs immediately before the septa on the main hypha, and the segment length is equal to the internodal distance, respectively 227, 236, and 256 μm for the three segments shown in **Figure 2b**. These values for the internodal distances are slightly larger than those of 179.29 ± 11.27 μm measured by Vidal-Diez et al. (2015).

One has to be careful in assigning values to the branching angles in the case of these experiments. Indeed, when growing on agar plates, fungal hyphae have a major incentive to branch out strictly at the surface of the agar, from which they derive energy and carbon. In the experiments described here, however, hyphae derive their sustenance strictly from the poppy seeds, and are therefore not bound metabolically to spread along the bottom surface of the micromodels, as they would be expected to do when growing in agar (even though, even in these cases, it is not infrequent to see them shoot upward as well). Inside the micromodels, branching hyphae can shoot upward at least
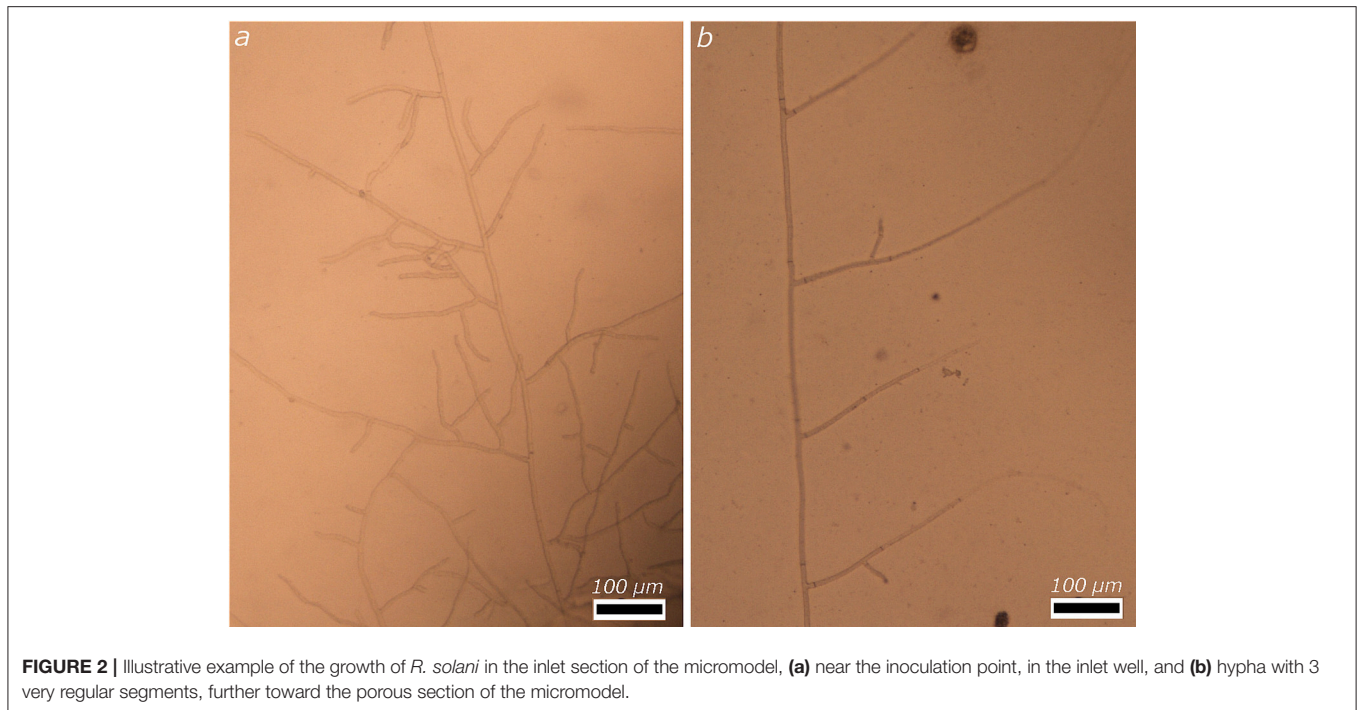
FIGURE 2 | Illustrative example of the growth of *R. solani* in the inlet section of the micromodel, **(a)** near the inoculation point, in the inlet well, and **(b)** hypha with 3 very regular segments, further toward the porous section of the micromodel.

initially, until they reach the 34 μm-high ceiling of the cavities inside the micromodels and are then forced to move horizontally or come back down. Analysis of the resulting images at too coarse a magnification gives the misleading impression of a branching angle that is very different than one would expect, when in fact, close analysis of the images shows sharp bends of the hyphae right after branching. This same process occurs within the microporous regions in the micromodels. In this article, whenever branching angles are mentioned, it is after careful evaluation of the branching at different focal distances of the microscope, to avoid gross misrepresentations.

Influence of Liquid Phase on Fungal Spread

After an initial period during which the hyphae propagate in the inlet regions of the channels, some hyphae tips reach the microporous region, which is variably saturated with distilled water. Based on previous observations by several authors (e.g., Otten et al., 1999), one anticipates at that point that the hyphae would tend to spread preferentially inside larger pores, which are not water filled. Indeed, this behavior is clearly evinced in our experiments (see **Figure 3**). Bundles of hyphae are seen in several images to converge to single air-filled pores and to grow there in preference to other portions of the pore space that are saturated with liquid. One needs to be careful in interpreting these observations because of the fact that the surface of the micromodels in the portions of the pores that are unsaturated are likely not to have properties similar to those of sand particles, because the plasma treatment of the PDMS is not permanent under these conditions. This point will need to be taken into account in future research. Be that as it may, the apparent preference for the unsaturated part of the pore space is not
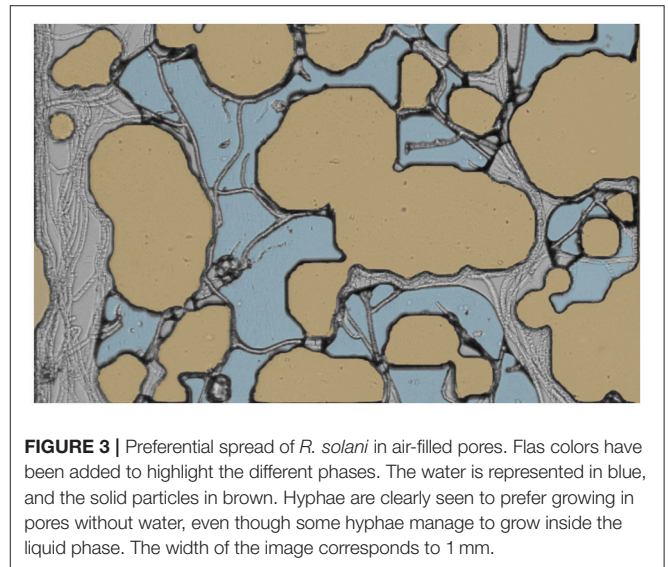

FIGURE 3 | Preferential spread of *R. solani* in air-filled pores. Flas colors have been added to highlight the different phases. The water is represented in blue, and the solid particles in brown. Hyphae are clearly seen to prefer growing in pores without water, even though some hyphae manage to grow inside the liquid phase. The width of the image corresponds to 1 mm.

exclusive. As many authors have pointed out, hyphae are capable of growing through water-filled space if need be, as seen in the water-filled parts of **Figure 3**. Indeed in a series of papers it was shown that *R. solani* used in this study spreads preferentially through water filled pores, larger pores and readily crosses cracks, but when given little choice does spread through smaller and water filled pores (Otten et al., 1999, 2004a,b).

Another feature that is manifested in this same image is the fact that, after a while, as the hyphae undoubtedly consume some of the liquid phase around them, or as the water slowly evaporates from the microcosms, the configuration of the liquid phase that

remains in the pores tends in places to adjust to the presence of the hyphae. Pockets of water exhibit external surfaces that appear to be unphysical from the standpoint of the theory of capillarity, e.g., with a concavity opposite to what one might expect based on the geometry of nearby solid surfaces. However, in many cases, these conflicting observations can be resolved once one realizes upon scrutiny of the micrographs that these interfaces are held in place by one or more fungal hyphae acting as a restraining net.

Linear Apical Extension and Growth Along Pore Walls

In many of the images of the water-saturated microporous regions of the micromodels, hyphae appear to be extending linearly for hundreds of microns without branching (**Figure 4**). Again, one needs to be very careful in that context, and make sure by changing the focal plane of the microscope that one does not miss branching that may occur vertically. But in the absence of such branching, the very long internodal distances that are apparent in these images are in sharp contrast with what has been routinely observed on agar plates.

When a hypha encounters a pore wall, as in **Figure 4** (at point b) and in **Figure 5** (at point a), there is a clear tendency for it to stay in contact with it for a while, as expected according to Watts et al. (1998), a phenomenon termed thigmotropism. This behavior is not entirely surprising and may be due in this case to some extent to electrostatic interactions. *R. solani* might react positively to electrical surface charge, as small as it might be (similar to that on sand particles) on the walls of the pillars in the micromodels. Common wisdom is that if one drags one's finger on a flat surface, producing static electricity in the process, fungal hyphae subsequently colonizing the surface will have a tendency to follow closely the path of the finger. By the same process, hyphae approaching a surface tangentially would have a tendency to keep following it closely afterwards, even if the surfaces curves. Nevertheless, it is clear from **Figures 4**, **5**, that this tendency does not associate the hyphae and surfaces indefinitely. At different stages in the progression of the hypha in **Figure 4**, and at point b in **Figure 5**, the hyphae begin to separate from the surfaces and eventually foray into the open pore space.

Hyphae Encountering Pore Walls "Head on"

Less predictable initially was what happens to fungal hyphae that run straight into a pore wall, as in **Figure 6**. As it touches the wall, the hypha in this image does not branch, as one might have expected. Instead, it seems to keep elongating. The apical region does not move, but the part of the hypha behind it progressively bends to accommodate the extra length that is generated over time. As the bending intensifies, the angle the apex makes with the surface reduces progressively, until the apex is eventually not encumbered by the surface any more, and can grow again, alongside it. This sequence of events, which is observed in many of the pictures we took, clearly deviates from the sequence of steps described by the model of Hopkins and Boswell (2012). In the presence of confining surfaces, fungal hyphae cannot be viewed as series of rigid, straight tubes connected with each other. Provision needs to be made in models for connected tubes to bend in response to constraints.

Branching Pattern

In a previous section, it was mentioned that hyphae can elongate sometimes more than a mm without branching (as in **Figure 4**), unlike what has been routinely observed on Petri dishes. This
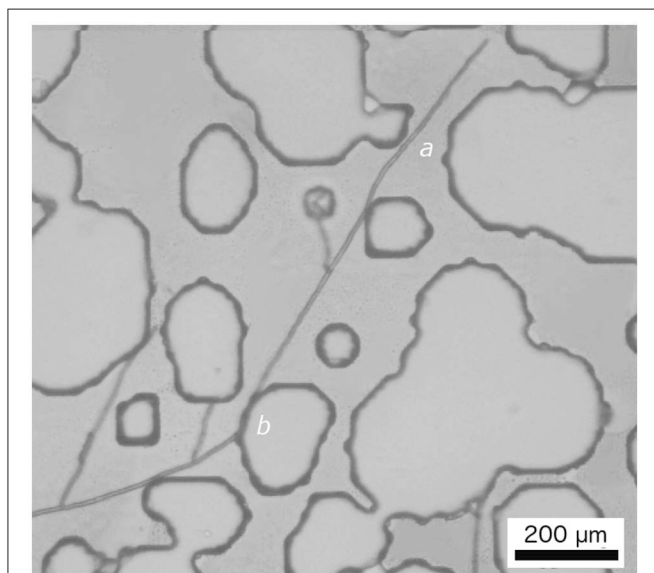
FIGURE 4 | Example of particularly long extension of hyphae in the water-saturated portion of the micromodel. (a) this very long hyphal segment does not show any appearance of branching yet, at the time the picture was taken. (b) At that point, the hypha touches the surface of the pore, and stays in contact with it for a little while, but eventually separates from the surface to return to the pore space.
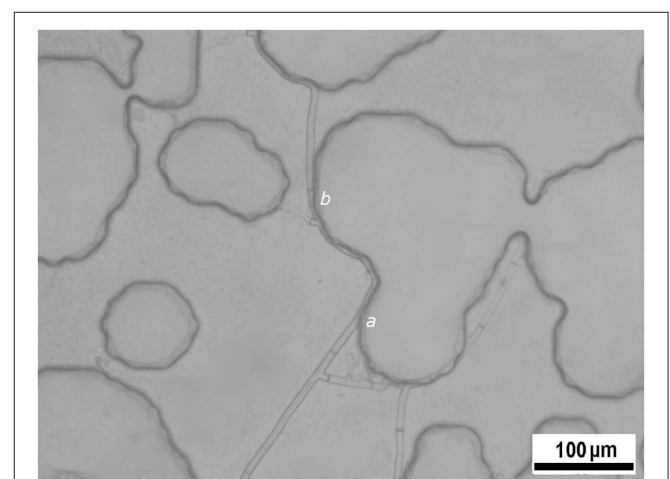
FIGURE 5 | Illustration of the tendency of hyphae to stay in close contact with pore walls once they encounter them (at point a). Nevertheless, this thigmotrophic process does not extend indefinitely, as the hypha eventually dissociates from the surface (at point b).
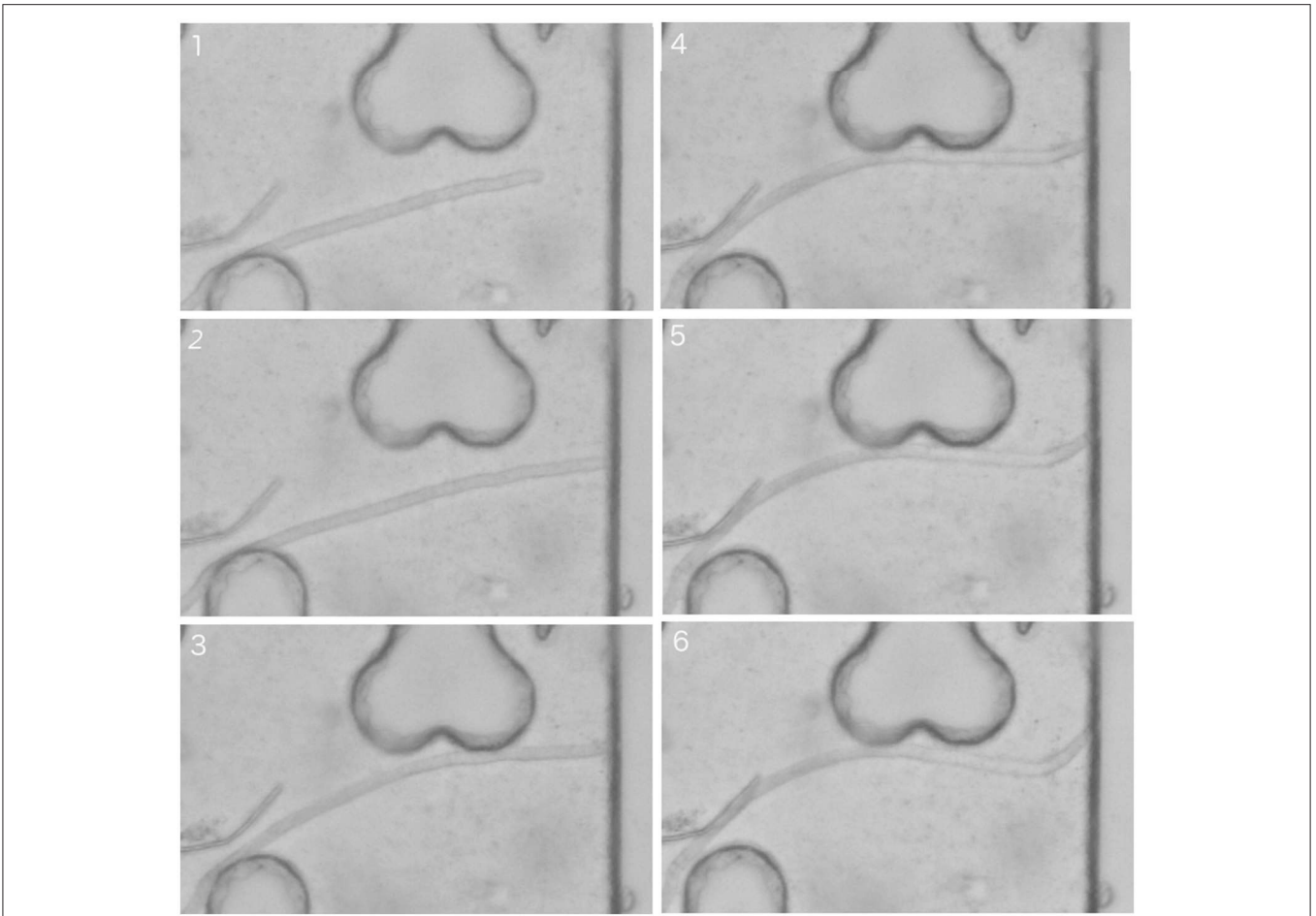
FIGURE 6 | Time sequence of 6 successive snapshots (1 to 6) of the propagation and bending of a hypha and its encounter "head on" with a pore wall.
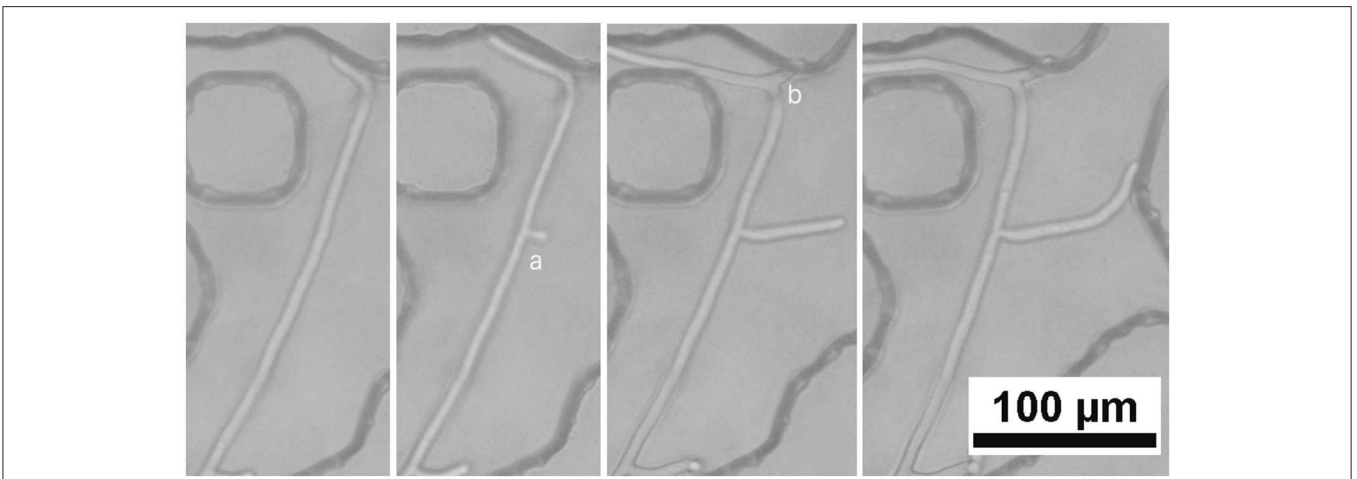

FIGURE 7 | Location and time sequence of the branching of a hypha. (a) at this point, immediately preceding a septum, branching seems to be very much like that observed in Petri dishes or in the inlet portion of the micromodel, whereas at (b) the branching seems to be closely associated with the strong bending of the hypha.

behavior may be due to the fact that hyphae in our experiments are surrounded by distilled water. There is therefore very little reason for the hyphae to branch out to scavenge more nutrients and energy from their environment. Nevertheless, hyphae do branch out at various times. Some of this branching, as in **Figure 7** at point "a," just before a septum, seems to be typical of what happens in Petri dish. But many cases of branching in the hundreds of images that we have taken seem to be as at point "b" in **Figure 7**, associated with bending of the hyphae, following a "head-on collision" with pore walls. The common explanation for the branching process, as mentioned earlier, is that it is related to turgor pressure inside the cell that eventually branch. Turgor pressure is a strictly osmotic process, related to the concentration of electrolyte inside the cytoplasm. However, it could be that the pressure felt inside the branching cell in soil pores is in fact more mechanical than osmotic. As the hypha elongates and is forced to bend, cells walls may be under sizeable stress, just as they would under regular turgor pressure.

CONCLUSION

The research described above corresponds to a first attempt to use a soil-like micromodel to identify the parameters that control the growth of fungal hyphae in the confining pore space of soils. The results suggest that *R. solani*, introduced in the micromodel on a poppy seed from which it subsequently propagates, is indeed able to penetrate into the microporous portion of the micromodel, without having to be enticed to do so. Once the fungus has penetrated inside the micromodel, a working hypothesis in the research was that the geometry of the pores, as well as the presence of hard surfaces in the path of the hyphae would influence the latter's behavior significantly. The experimental results support this hypothesis. Indeed, both the branching pattern as well as the apical elongation of the hyphae appear to be strongly affected by the presence of "obstacles" in soil pores. In particular, far from being series of straight and rigid tubes, hyphae of *R. solani* are able to bend after the forward movement of the apex has stopped. The observations reported in this article therefore suggest that the modeling of hyphal growth in soils cannot simply be viewed as a special case of growth in more open environments. A model tailored to soils will have to encompass very different growth mechanisms and characteristics.

This preliminary experiment shows that it is feasible to use micromodels to study the behavior of fungi under conditions that, although nearly 2-dimensional, are in many respects like those found in real soils. It will be interesting, in future experiments, to try to grasp better, quantitatively, the different parameters that control the growth of *R. solani*, and other fungi as well, in soil pores. This will require systematic replication so that statistics can be computed and the behavior of hyphae characterized in great detail. Further experiments could also address other aspects of the spread of fungal hyphae about which little is yet known, like what happens when different fungal species propagate in the same pore space in a soil, or when bacteria, hopping onto the external surfaces of hyphae, are carried along as the hyphae grows (a process often referred to as "hitchhiking on the fungal highway"). Clearly, there are a lot of avenues that can be pursued in this general context, all of which would result in a far better understanding than is currently available of the ecology of fungi in terrestrial environments.

AUTHOR CONTRIBUTIONS

ACKNOWLEDGMENTS

REFERENCES

Baveye, P. C. (2015). Grand challenges in the research on soil processes. *Front. Environ. Sci.* 3:10. doi: 10.3389/fenvs.2015.00010

Baveye, P. C., Otten, W., Kravchenko, A., Balseiro Romero, M., Beckers, É., Chalhoub, M., et al. (2018). Emergent properties of microbial activity in heterogeneous soil microenvironments: different research approaches are slowly converging, yet major challenges remain. *Front. Microbiol.* 8:1364. doi: 10.3389/fmicb.2017.01364

Baveye, P., Vandevivere, P., Hoyle, B. L., DeLeo, P. C., and de Lozada, D. S. (1998). Environmental impact and mechanisms of the biological clogging of saturated soils and aquifer materials. *Crit. Rev. Environ. Sci. Technol.* 28, 123–191. doi: 10.1080/10643389891254197

Boddy, L. (1993). Saprotrophic cord-forming fungi: warfare strategies and other ecological aspects. *Mycol. Res.* 97, 641–655. doi: 10.1016/S0953-7562(09)80141-X

Boswell, G. P., and Davidson, F. A. (2012). Modelling hyphal networks. *Fungal Biol. Rev.* 26, 30–38. doi: 10.1016/j.fbr.2012.02.002

Boswell, G. P., and Hopkins, S. (2008). Linking hyphal growth to colony dynamics: spatially explicit models of mycelia. *Fungal Ecol.* 1, 143–154. doi: 10.1016/j.funeco.2008.10.003

Cazelles, K., Otten, W., Baveye, P. C., and Falconer, R. E. (2013). Soil fungal dynamics: parameterisation and sensitivity analysis of modelled physiological processes, soil architecture and carbon distribution. *Ecol. Modell.* 248, 165–173. doi: 10.1016/j.ecolmodel.2012.08.008

Choudhury, M. J. A., Trevelyan, P. M. J., and Boswell, G. P. (2018). A mathematical model of nutrient influence on fungal competition. *J. Theor. Biol.* 438, 9–20. doi: 10.1016/j.jtbi.2017.11.006

Cromack, K., and Caldwell, B. A. (1992). "The role of fungi in litter decomposition and nutrient cycling," in *The Fungal Community — Its Organization and Role in the Ecosystem,* eds G. C. Carroll and D. T. Wicklow (New York, NY: Marcel Dekker), 653–668.

Cruz, B. C., Furrer, J. M., Guo, Y. S., Dougherty, D., Hinestroza, H. F., Hernandez, J. S., et al. (2017). Pore-scale water dynamics during drying and the impacts of structure and surface wettability. *Water Resour. Res.* 53, 5585–5600. doi: 10.1002/2016WR019862

Deng, J., Orner, E. P., Chau, F., Anderson, E. M., Kadilak, A. L., Rubinstein, R. L., et al. (2015). Synergistic effects of soil microstructure and bacterial EPS on drying rate in emulated soil micromodels. *Soil Biol. Biochem.* 83, 116–124. doi: 10.1016/j.soilbio.2014.12.006

Falconer, R. E., Battaia, G., Schmidt, S., Baveye, P., Chenu, C., and Otten, W. (2015). Microscale heterogeneity explains experimental variability and non-linearity in soil organic matter mineralisation. *PLoS ONE* 10:e0123774. doi: 10.1371/journal.pone.0123774

Falconer, R. E., Houston, A. N., Otten, W., and Baveye, P. C. (2012). Emergent behavior of soil fungal dynamics: influence of soil architecture and water distribution. *Soil Sci.* 177, 111–119. doi: 10.1097/SS.0b013e31824 1133a

Fisher, M. C., Henk, D. A., Briggs, C. J., Brownstein, J. S., Madoff, L. C., McCraw, S. L., et al. (2012). Emerging fungal threats to animal, plant and ecosystem health. *Nature* 484:186. doi: 10.1038/nature10947.

Foster, R. C. (1988). Microenvironments of soil microorganisms. *Biol. Fertil. Soils* 6, 189–203.

Fricker, M. D., Heaton, L. L. M., Jones, N. S., and Boddy, L. (2017). The mycelium as a network. *Microbiol. Spect.* 5. doi: 10.1128/microbiolspec.FUNK-0033-2017

Fries, N. (1973). Effects of volatile organic compounds on the growth and development of fungi. *Trans. Br. Mycol. Soc.* 60, 1–21. doi: 10.1016/S0007-1536(73)80055-5

Gow, N. A., and Gadd, G. M. (1995). *The Growing Fungus.* London: Chapman and Hall.

Hanson, K. L., Nicolau, D. V. Jr., Filipponi, L., Wang, L., Lee, A. P., and Nicolau, D. V. (2006). Fungi use efficient algorithms for the exploration of microfluidic networks. *Small* 2, 1212–1220. doi: 10.1002/smll.2006 00105

Harris, K., Crabb, D., Young, I. M., Weaver, H., Gilligan, C. A., Otten, W., et al. (2002). *In situ* visualisation of fungi in soil thin sections: Problems with crystallisation of the fluorochrome FB 28 (CalcofluorM2R) and improved staining by SCRI Renaissance 2200. *Mycol. Res.* 106, 293–297. doi: 10.1017/S0953756202005749

Harris, K., Young, I. M., Gilligan, C. A., Otten, W., and Ritz, K. (2003). Effect of bulk density on the spatial organisation of the fungus R. solani in soil. *Fems Microbiol. Ecol.* 44, 45–56. doi: 10.1111/j.1574-6941.2003. tb01089.x

Hawksworth, D. L. (2001). The magnitude of fungal diversity: the 1.5 million species estimate revisited* *Paper presented at the Asian Mycological Congress 2000 (AMC 2000), incorporating the 2nd Asia-Pacific Mycological Congress on Biodiversity and Biotechnology, and held at the University of Hong Kong on 9-13 July 2000. *Mycol. Res.* 105, 1422–1432. doi: 10.1017/S09537562010 04725

Held, M., Edwards, C., and Nicolau, D. V. (2011). Probing the growth dynamics of Neurospora crassa with microfluidic structures. *Fungal Biol.* 115, 493–505. doi: 10.1016/j.funbio.2011.02.003

Held, M., Lee, A. P., Edwards, C., and Nicolau, D. V. (2010). Microfluidics structures for probing the dynamic behaviour of filamentous fungi. *Microelectron. Eng.* 87, 786–789. doi: 10.1016/j.mee.2009. 11.096

Hopkins, S., and Boswell, G. P. (2012). Mycelial response to spatiotemporal nutrient heterogeneity: a velocity-jump mathematical model. *Fungal Ecol.* 5, 124–136. doi: 10.1016/j.funeco.2011.06.006

Jia, X., and Williams, R. A. (2001). A packing algorithm for particles of arbitrary shapes. *Powder Technol.* 120, 175–186. doi: 10.1016/S0032-5910(01) 00268-6

Karadimitriou, N. K., and Hassanizadeh, S. M. (2012). A review of micromodels and their use in two-phase flow studies. *Vadose Zone Journal* 11. doi: 10.2136/vzj2011.0072.

Koebernick, N., Daly, K. R., Keyes, S. D., George, T. S., Brown, L. K., Raffan, A., et al. (2017). High-resolution synchrotron imaging shows that root hairs influence rhizosphere soil structure formation. *New Phytol.* 216, 124–135. doi: 10.1111/nph.14705

Lilje, O., Lilje, E., Marano, A. V., and Gleason, F. H. (2013). Three dimensional quantification of biological samples using micro-computer aided tomography (microCT). *J. Microbiol. Methods* 92, 33–41. doi: 10.1016/j.mimet.2012. 10.006

Miller, R. M., and Jastrow, J. D. (2000). "Mycorrhizal fungi influence soil structure," in *Arbuscular Mycorrhizas: Physiology and Function*, eds Y. Kapulnik and D. D. Douds (Dordrecht: Springer), 3–18.

Otten, W., and Gilligan, C. A. (1998). Effect of physical conditions on the spatial and temporal dynamics of the soil-borne fungal pathogen *Rhizoctonia solani*. *New Phytol.* 138, 629–637.

Otten, W., Bailey, D. J., and Gilligan, C. A. (2004a). Empirical evidence of spatial thresholds to control invasion of fungal parasites and saprotrophs. *New Phytol.* 163, 125–132. doi: 10.1111/j.1469-8137.2004. 01086.x

Otten, W., Gilligan, C. A., Watts, C. W., Dexter, A. R., and Hall, D. (1999). Continuity of air-filled pores and invasion thresholds for a soilborne fungal plant pathogen, *R. solani. Soil Biol. Biochem.* 31, 1803–1810. doi: 10.1016/s0038-0717(99)00099-1

Otten, W., Hall, D., Harris, K., Ritz, K., Young, I. M., and Gilligan, C. A. (2001). Soil physics, fungal epidemiology and the spread of *R. solani. New Phytol.* 151, 459–468. doi: 10.1046/j.0028-646x.2001. 00190.x

Otten, W., Harris, K., Young, I. M., Ritz, K., and Gilligan, C. A. (2004b). Preferential spread of the pathogenic fungus *R. solani* through structured soil. *Soil Biol. Biochem.* 36, 203–210. doi: 10.1016/j.soilbio.2003. 09.006

Otten, W., Pajor, R., Schmidt, S., Baveye, P. C., Hague, R., and Falconer, R. E. (2012). Combining X-ray CT and 3D printing technology to produce microcosms with replicable, complex pore geometries. *Soil Biol. Biochem.* 51, 53–55. doi: 10.1016/j.soilbio.2012. 04.008

Pajor, R., Falconer, R., Hapca, S., and Otten, W. (2010). Modelling and quantifying the effect of heterogeneity in soil physical conditions on fungal growth. *Biogeosciences* 7, 3731–3740. doi: 10.5194/bg-7-3731-2010

Paulitz, T. C., and Schroeder, K. L. (2005). A new method for the quantification of *R. solani* and *R. oryzae* from soil. *Plant Dis.* 89, 767–772. doi: 10.1094/PD-89-0767

Riquelme, M., and Bartnicki-Garcia, S. (2004). Key differences between lateral and apical branching in hyphae of *Neurosora crassa*. *Fungal Genet. Biol.* 41, 842–851. doi: 10.1016/j.fgb.2004.04.006

Riquelme, M., Reynaga-Peña, C. G., Gierz, G., and Bartnicki-García, S. (1998). What determines growth direction in fungal hyphae? *Fungal Genet. Biol.* 24, 101–109. doi: 10.1006/fgbi.1998.1074

Roman, G. T., and Culbertson, C. T. (2006). Surface engineering of poly(dimethylsiloxane) microfluidic devices using transition metal sol–gel chemistry. *Langmuir* 22, 4445–4451. doi: 10.1021/la 053085w

Rubinstein, R. L., Kadilak, A. L., Cousens, V. C., Gage, D. J., and Shor, L. M. (2015). Protist-facilitated particle transport using emulated soil micromodels. *Environ. Sci. Technol.* 49, 1384–1391. doi: 10.1021/es50 3424z

Sposito, G. (2013). Green water and global food security. *Vadose Zone J.* 12. doi: 10.2136/vzj2013.02.0041

Stamets, P. (2005). *Mycelium Running: How Mushrooms Can Help Save the World.* Berkeley, CA: Ten Speed Press.

Stanley, C. E., Grossmann, G., Casadevall i Solvas, X., and deMello, A. J. (2016). Soil-on-a-Chip: microfluidic platforms for environmental organismal studies. *Lab Chip* 16, 228–241. doi: 10.1039/C5LC0 1285F.

Vidal-Diez de Ulzurrun, G., Baetens, J. M., Van den Bulcke, J., and De Baets, B. (2017). Modelling three-dimensional fungal growth in response to environmental stimuli. *J. Theor. Biol.* 414, 35–49. doi: 10.1016/j.jtbi.2016.11.020

Vidal-Diez de Ulzurrun, G., Baetens, J. M., Van den Bulcke, J., Lopez-Molina, C., De Windt, I., and De Baets, B. (2015). Automated image-based analysis of spatio-temporal fungal dynamics. *Fungal Genet. Biol.* 84, 12–25. doi: 10.1016/j.fgb.2015.09.004

Watts, H. J., Véry, A. A., Perera, T. H., Davies, J. M., and Gow, N. A. (1998). Thigmotropism and stretch-activated channels in the pathogenic fungus *Candida albicans*. *Microbiology* 144 (Pt 3), 689–695. doi: 10.1099/00221287-144-3-689